Neuron, Vol. 44, 977–986, December 16, 2004, Copyright ©2004 by Cell Press

Huntingtin-Interacting Protein HIP14 Is a Palmitoyl Transferase Involved in Palmitoylation and Trafficking of Multiple Neuronal Proteins

Kun Huang,[1,4] Anat Yanai,[2,4] Rujun Kang,[1,4] Pamela Arstikaitis,[1] Roshni R. Singaraja,[2] Martina Metzler,[2] Asher Mullard,[1] Brendan Haigh,[2] Catherine Gauthier-Campbell,[1] Claire-Anne Gutekunst,[3] Michael R. Hayden,[2,*] and Alaa El-Husseini[1,*]

[1]Department of Psychiatry
Brain Research Centre
University of British Columbia
Vancouver, British Columbia
Canada

[2]Center for Molecular Medicine and Therapeutics
Department of Medical Genetics
Children's and Women's Hospital
Vancouver, British Columbia
Canada

[3]Department of Neurology
Emory University
Atlanta, Georgia 30329

Summary

In neurons, posttranslational modification by palmitate regulates the trafficking and function of signaling molecules, neurotransmitter receptors, and associated synaptic scaffolding proteins. However, the enzymatic machinery involved in protein palmitoylation has remained elusive. Here, using biochemical assays, we show that huntingtin (htt) interacting protein, HIP14, is a neuronal palmitoyl transferase (PAT). HIP14 shows remarkable substrate specificity for neuronal proteins, including SNAP-25, PSD-95, GAD65, synaptotagmin I, and htt. Conversely, HIP14 is catalytically invariant toward paralemmin and synaptotagmin VII. Exogenous HIP14 enhances palmitoylation-dependent vesicular trafficking of several acylated proteins in both heterologous cells and neurons. Moreover, interference with endogenous expression of HIP14 reduces clustering of PSD-95 and GAD65 in neurons. These findings define HIP14 as a mammalian palmitoyl transferase involved in the palmitoylation and trafficking of multiple neuronal proteins.

Introduction

Trafficking of proteins to specialized subcellular and plasma membrane domains is vital for normal cell development and function (Da Silva and Dotti, 2002; Lee and Sheng, 2000). Modification by the lipid palmitate, a 16 carbon fatty acid chain, influences sorting and function of several proteins (Linder and Deschenes, 2004; Smotrys and Linder, 2004). In particular, palmitoylation has recently emerged as a critical modification in neurons where it controls axon pathfinding, filopodia formation, polarized protein targeting, and clustering of scaffolding and signaling proteins (El-Husseini and Bredt, 2002; Gauthier-Campbell et al., 2004; Strittmatter et al., 1995; Ueno, 2000).

Postsynaptic targeting and clustering of the postsynaptic density (PSD) protein PSD-95 requires palmitoylation, and this process regulates glutamate receptor retention at the synapse (Craven et al., 1999). Palmitoylation also regulates SNAP-25-mediated SNARE complex disassembly, presynaptic targeting of the GABA synthesizing enzyme GAD65, multimerization, and presynaptic trafficking of the calcium sensor synaptotagmin I (Chapman et al., 1996; Fukuda et al., 2001; Kanaani et al., 2002; Kang et al., 2004; Rathenberg et al., 2004; Washbourne et al., 2001). In addition, palmitoylation of secreted proteins regulates neuronal differentiation (Chamoun et al., 2001; Linder and Deschenes, 2004). Remarkably, physiological stimuli and neuronal activity dynamically alter protein palmitoylation levels, and this provides an important mechanism for the regulation of neuronal cell development and activity (El-Husseini et al., 2002; Resh, 1999; Smotrys and Linder, 2004).

While the importance of palmitoylation in protein trafficking is well documented, the palmitoyl transferases involved in this process remain unknown (Smotrys and Linder, 2004). The diversity of sequences modified by palmitate hindered the identification of these enzymes using classical protein purification approaches. A significant advance in the field came from genetic analysis in yeast, which revealed a family of PATs that contains a DHHC domain, a cysteine rich region that harbors a conserved tetra-peptide motif. These include Erf2p/Erf4p protein complex, which palmitoylate H-Ras proteins, and Akr1p, which is involved in the palmitoylation of the yeast casein kinase Yck2p (Linder and Deschenes, 2004; Roth et al., 2002). However, it remained unknown whether related proteins served a similar function in mammalian cells. Here, we use biochemical assays to show that huntingtin-interacting protein, HIP14, is a neuronal palmitoyl transferase involved in the palmitoylation of specific substrates. We also show that HIP14 modulates palmitoylation-dependent vesicular trafficking and clustering of a subset of synaptic proteins.

Results

HIP14 Is a Neuronal Palmitoyl Transferase

HIP14, a mammalian ortholog of Akr1p, was previously identified as an htt-interacting protein involved in regulating protein trafficking (Singaraja et al., 2002). This protein is predominantly expressed in neurons in the brain and localizes to Golgi membranes and cytoplasmic vesicles (Singaraja et al., 2002). Structurally, HIP14 contains five predicted transmembrane domains and a DHHC domain similar to that seen in yeast PATs (Figure 1A). These observations prompted us to test whether HIP14 is involved in the palmitoylation of several neuronal proteins.

First, we coexpressed HIP14 with SNAP-25, a well-

*Correspondence: alaa@interchange.ubc.ca (A. E.-H.); mrh@cmmt.ubc.ca (M.H.)

[4]These authors contributed equally to this work.

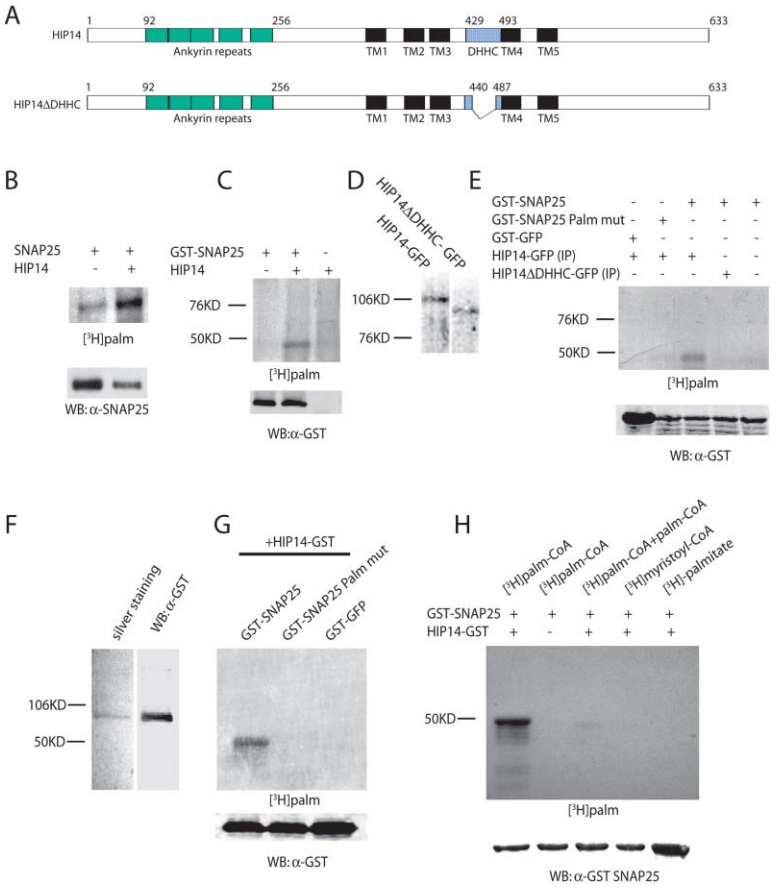

Figure 1. HIP14 Is a Neuronal Palmitoyl Transferase

(A) Schematic illustration of HIP14 primary structure. HIP14 lacking the DHHC domain (HIP14ΔDHHC) was generated by deletion of amino acids 440–487 containing the cysteine-rich zinc finger domain.

(B) Enhancement of SNAP-25 palmitoylation in vivo by HIP14. COS cells were transfected either with SNAP-25 alone or with HIP14. Eight hours posttransfection, cells were metabolically labeled with [^{3}H]palmitate, and SNAP-25 was immunoprecipitated and analyzed by Western blotting (WB) and autoradiography ([^{3}H]palm). SNAP-25 palmitoylation levels were enhanced in cells coexpressing HIP14.

(C) Extracts of COS cells transfected with HIP14 induce palmitoylation of purified GST-SNAP-25 in the presence of [^{3}H]palmitoyl-CoA.

(D and E) COS cells were transfected with GFP fusion of either wild-type HIP14 (HIP14-GFP) or the mutant form lacking the DHHC domain (HIP14ΔDHHC GFP). GFP fusion proteins were then immunoprecipitated (IP) using GFP antibodies. HIP14 GFP (IP) induced palmitoylation of wild-type (GST-SNAP-25) but not the palmitoylation mutant form of SNAP25 (GST-SNAP-25 Palm mut) or GST-GFP. In contrast, HIP14ΔDHHC failed to palmitoylate GST-SNAP-25.

(F and G) Purified HIP14-GST is sufficient to induce palmitoylation of GST-SNAP-25. HIP14-GST produced in bacteria was purified, and samples were subjected to Western blotting and silver staining. No palmitoylated products were detected when GST-SNAP-25 Palm mut or GST-GFP were incubated with HIP14-GST.

(H) Acylation mediated by HIP14 requires palmitoyl-CoA. HIP14 requires [^{3}H]palmitoyl-CoA but not [^{3}H]palmitate for SNAP-25 palmitoylation. This reaction was competed with excess cold palmitoyl-CoA. HIP14 did not induce transfer of the lipid myristate from [^{3}H]myristoyl-CoA.

characterized palmitoylated neuronal protein (Gonzalo and Linder, 1998; Hess et al., 1992), followed by metabolic labeling with [^{3}H]palmitate. These experiments demonstrated that SNAP-25 palmitoylation was potentiated in the presence of HIP14, suggesting that SNAP-25 may serve as a substrate for this putative enzyme (Figure 1B). Next, several in vitro assays were performed to determine if the enzymatic reaction was directly mediated by HIP14. Purified GST-SNAP-25 was incubated with extracts obtained from COS cells transfected with wild-type HIP14 in the presence of [^{3}H]palmitoyl-CoA, and this induced palmitoylation of SNAP-25 (Figure 1C). In contrast, lysates containing HIP14 failed to palmitoylate a mutant form of SNAP-25 lacking the cysteines normally modified by palmitate.

Consistent with the postulated role for the DHHC domain in PAT activity, we also found that a mutant form of HIP14 lacking this domain failed to catalyze palmitoylation of SNAP-25. To further characterize the role of HIP14, GST-SNAP-25 was incubated with HIP14 GFP immunoprecipitates (IP) obtained from transfected cells to determine whether HIP14 was sufficient for SNAP-25 palmitoylation. In vitro labeling assays showed that SNAP-25 palmitoylation occurs only in the presence of wild-type but not a mutant form of HIP14 lacking the DHHC domain (Figures 1D and 1E). To determine whether purified HIP14 was sufficient to induce protein palmitoylation, a HIP14-GST fusion protein was generated in bacteria and then purified using glutathione beads. The eluted protein was used in an in vitro assay in the presence or absence of [^{3}H]palmitoyl-CoA (Figures 1F–1H). Indeed, purified HIP14-GST was sufficient to palmitoylate GST-SNAP-25 in the presence of [^{3}H]palmitoyl-CoA but not [^{3}H]palmitate, and this reaction was completed by addition of excess nonradiolabeled palmitoyl-CoA (Figure 1H). To further characterize the specificity of this enzyme in this reaction, we next evaluated whether purified HIP14-GST mediates the transfer of other lipids, such as myristate. However, in the presence of [^{3}H]myristoyl-CoA, HIP14 failed to modify GST-SNAP-25 with myristate (Figure 1H). These findings establish that HIP14 utilizes palmitoyl-CoA to specifically modify SNAP-25 with palmitate on cysteine residues normally modified by this lipid in vivo.

Multiple Neuronal Proteins Serve as Substrates for HIP14

Previous work established that the postsynaptic density protein PSD-95 was palmitoylated at two N-terminal cysteines present at positions 3 and 5 and that this lipid modification was required for the trafficking of PSD-95 to the synapse (Craven et al., 1999; El-Husseini et al., 2000). To test whether HIP14 may also palmitoylate

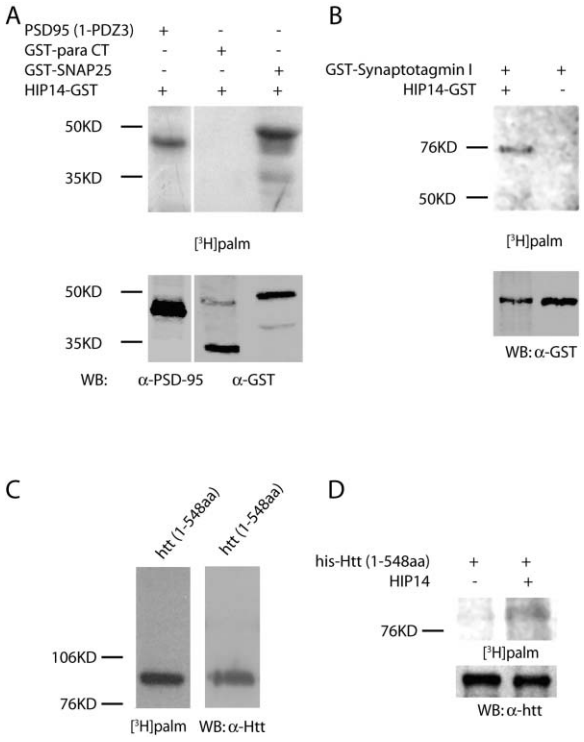

Figure 2. HIP14 Palmitoylates Multiple Substrates

(A) HIP14-GST induces palmitoylation of purified PSD-95 (1-PDZ3) and GST-SNAP-25, but not the dually acylated motif of paralemmin (GST-para CT).

(B) Palmitoylation of GST fusion protein of synaptotagmin I (GST-synaptotagmin I) by purified HIP14-GST.

(C) Htt is palmitoylated in vivo. COS cells transfected with the N-terminal fragment of htt containing amino acids 1–548 (htt [1–548aa]) were metabolically labeled with [^{3}H]palmitate and palmitoylation of immunoprecipitated Htt (1–548aa) was analyzed by Western blotting (WB) and autoradiography ([^{3}H]palm).

(D) Htt is a substrate for HIP14. Purified His-Htt (1–548aa) was palmitoylated in the presence of COS cell extracts expressing HIP14.

PSD-95, we first generated a GST fusion protein of PSD-95 containing the N-terminal amino acids 1–385, which contains the palmitoylation motif and PDZ domains 1–3 [PSD-95 (1-PDZ3)]. Because PSD-95 palmitoylation requires a free N terminus, GST was cleaved and a purified PSD-95 (1-PDZ3) was obtained. Both extracts from COS cells transfected with HIP14 as well as purified HIP14-GST induced PSD-95 palmitoylation in vitro (Figure 2A and see Supplemental Figure S1 [http://www.neuron.org/cgi/content/full/44/6/977/DC1/]).

To further analyze the role of HIP14 in the acylation of other neuronal proteins, we preformed in vitro assays on GST fusion proteins of synaptotagmin I and acylated sequences of GAD65, H-Ras, lck, paralemmin, and synaptotagmin VII. This analysis showed that HIP14-GST can also palmitoylate GST-synaptotagmin I, a presynaptic vesicle protein palmitoylated on 5 cysteine residues (Cys-74, Cys-75, Cys-77, Cys-79, and Cys-82) present in the junction between the transmembrane and cytoplasmic region of synaptotagmin I (Heindel et al., 2003; Sudhof, 2002) (Figure 2B). HIP14 also modified sequences of GAD65 containing the N-terminal palmitoylation motif (Supplemental Figure S1C [http://www.neuron.org/cgi/content/full/44/6/977/DC1/]). However, HIP14 did not palmitoylate the C-terminal motif of the dually palmitoylated and prenylated neuronal protein paralemmin (Kutzleb et al., 1998) (Figure 2A). Moreover, HIP14 did not induce palmitoylation of acylated sequences of H-Ras, lck, or synaptotagmin VII (Supplemental Figure S1C). These results indicate that HIP14 is involved in the palmitoylation of a specific subset of neuronal proteins.

The association of N-terminal sequences of htt (amino acids 1–548) with HIP14 suggested that htt was also a substrate for HIP14. Metabolic labeling analysis showed that the N-terminal region of htt was subject to palmitoylation (Figure 2C). Using a similar in vitro assay to the one described for SNAP-25, we also found that extracts of COS cells expressing HIP14 induced the palmitoylation of purified His-tagged htt (Figure 2D). These results demonstrate that htt is another substrate subject to palmitoylation by HIP14.

In addition to modifying several substrates with palmitate, metabolic labeling studies show that HIP14 itself is palmitoylated and that this process relies on the presence of its DHHC domain (Supplemental Figure S2A [http://www.neuron.org/cgi/content/full/44/6/977/DC1/]). These findings indicate that, akin to Akr1p, acylation of the DHHC domain within HIP14 may also be required for the enzyme activity. Interestingly, deletion of the DHHC domain disrupted accumulation of HIP14 in the Golgi and resulted in a diffuse localization of this protein in the soma and dendrites (Supplemental Figure S2B). Thus, the DHHC domain also appears to contribute to the proper folding and/or trafficking of HIP14.

HIP14 Associates with Multiple Vesicular Compartments

Previous studies showed that endogenous HIP14 is localized to Golgi and in vesicles located in the cytoplasm (Singaraja et al., 2002). Double labeling analysis performed in NT2 cells showed that HIP14 is partially colocalized with the recycling and late endosomal markers Rab7 and Rab8. In contrast, HIP14-positive puncta did not significantly overlap with the early endosomal marker Rab5 or the adaptor protein AP2 (Supplemental Figure S3 [http://www.neuron.org/cgi/content/full/44/6/977/DC1/]). Electron microscopic (EM) analysis revealed that HIP14 was associated with the cytosolic side of diverse vesicular structures present in the soma and dendrites (Figures 3A–3G). In addition, immunogold particles were observed in dendritic spines and at the plasma membrane (Figure 3 and data not shown). Taken together, these results indicate that HIP14 associates with several vesicular structures, including the Golgi as well as sorting/recycling and late endosomal structures.

In cultured hippocampal neurons, HIP14 show prominent staining in a perinuclear compartment that significantly colocalizes with the Golgi marker GM-130 (Figure 3H). Similar distribution was also observed in COS cells transfected with HIP14 GFP (Figure 3I). Time-lapse imaging of COS cells transfected with HIP14 GFP, showed that HIP14 traffics in tubulovesicular structures budding from the perinuclear compartment (Figure 3J and Movie S1 [http://www.neuron.org/cgi/content/full/44/6/977/DC1/]). Moreover, vesicular structures containing SNAP-25 GFP and HIP14 DsRed were seen undergoing rapid

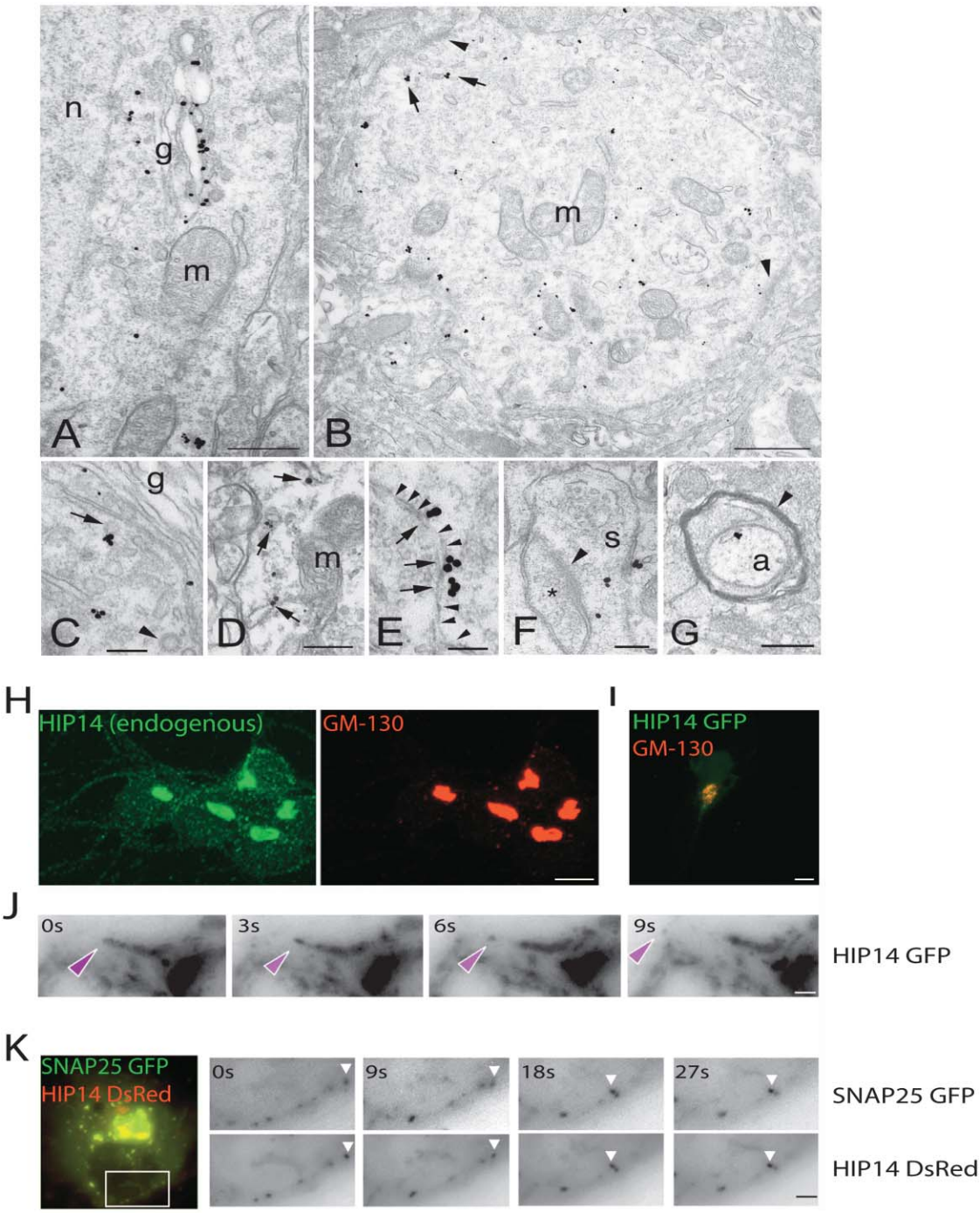

Figure 3. Association of HIP14 with Golgi and Cytoplasmic Vesicles

(A–G) Electron micrographs showing the subcellular localization of HIP14. (A) Micrograph showing a portion of neuronal perikarya. HIP14 immunogold particles are mostly decorating the cytoplasmic side of the Golgi stacks. (B) Micrograph showing HIP14 immunogold particles in a large-caliber dendrite receiving synaptic contacts (arrowheads). Immunogold particles are either free in the cytoplasm or associated with tubulovesicular elements (arrows). (C) Micrograh showing HIP14 immuogold particles associated with a coated vesicle (arrow) near the Golgi apparatus. A nonlabeled vesicle is also visible (arrowhead). (D) Micrograph of HIP14 immunogold particles associated with the cytoplasmic side of tubulovesicular elements (arrows) near the plasma membrane in the perikarya of a neuron. (E) HIP14 immunogold particles (arrows) associated with the plasma membrane (outlined by the arrowheads). (F) Micrograph showing HIP14 immunogold particles in the neck of a dendritic spine (s) receiving a synaptic contact (arrowhead) from an axon terminal (star). (G) HIP14 immunogold in an axon (a) surrounded by myelin (arrowhead). (H) HIP14 is mainly localized to the Golgi and cytoplasmic vesicles in hippocampal neurons. Hippocampal neurons (DIV 8) were stained for HIP14 and the Golgi marker GM-130. HIP14 accumulates in a perinuclear region positive for GM-130 and in small puncta throughout the cytoplasm. (I) Colocalization of HIP14 GFP and GM-130 in COS cells. (J) Tubulovesicular-like structures (arrowheads) containing HIP14 GFP budding from the perinuclear region in COS cells. Inverse color time-lapse images are shown. (K) HIP14 DsRed and SNAP-25 GFP colocalize in the perinuclear region and cytoplasmic vesicles. Time-lapse images show trafficking of both HIP14 DsRed and SNAP-25

transport in the cytoplasm (Figure 3K). These results indicate that HIP14 is involved in the cytosolic modification of both cytoplasmic and integral membrane proteins. Moreover, HIP14 in all likelihood modifies substrates at several subcellular locations.

Palmitoylation-Dependent Trafficking Is Regulated by HIP14

Palmitoylation is essential for vesicular trafficking of several proteins, including PSD-95, GAP-43, and SNAP-25, and usually results in the accumulation of these proteins in a compartment located in a perinuclear region (El-Husseini and Bredt, 2002; El-Husseini et al., 2000). Hence, we used this approach to assess the effects of HIP14 on the trafficking of these putative substrates in both heterologous cells and neurons. This analysis revealed that exogenous HIP14 enhanced perinuclear accumulation of PSD-95 and SNAP-25 (Figure 4, Table 1, and Supplemental Figure S4 [http://www.neuron.org/cgi/content/full/44/6/977/DC1/]). Enhanced perinuclear accumulation was also observed for some of the other proteins examined, including GAP-43, GAD65, and synaptotagmin I. In contrast, HIP14 did not alter the distribution of paralemmin and synaptotagmin VII or the palmitoylation-deficient forms of SNAP-25 and PSD-95 (Table 1). Consistent with these findings, metabolic labeling studies in heterologous cells showed that expression of HIP14 enhanced palmitoylation of synaptotagmin I, GAP-43, and SNAP-25 by 30%–50%. However, no change in the palmitoylation of synaptotagmin VII was observed (data not shown). The strong correlation between altered protein trafficking in vivo and protein acylation in both heterologous cells and in vitro assays indicates an important role for HIP14 in the acylation of several proteins in neurons.

Previous work has established that palmitoylation is important for trafficking of neuronal proteins to either the presynaptic or postsynaptic compartment. Specifically, palmitoylation is essential for postsynaptic targeting of PSD-95 (El-Husseini et al., 2000). When expressed in developing neurons, PSD-95 forms clusters that can be detected 12 hr posttransfection (El-Husseini et al., 2000). The number of clusters is gradually increased in the following 2–3 days. To assess whether HIP14 can modulate palmitoylation-dependent PSD-95 trafficking, we compared changes in PSD-95 GFP clustering 12–14 hr posttransfection when expressed alone or with HIP14. Figure 5A shows that expression of HIP14 specifically enhanced clustering of wild-type PSD-95 but did not alter the distribution of the palmitoylation-deficient form of PSD-95 or PSD-95 fused to a prenylated motif. These results are consistent with the proposed role for HIP14 in palmitoylation and trafficking of PSD-95 in neurons.

To further address whether endogenous HIP14 is important for palmitoylation-dependent trafficking of neuronal proteins, we generated a small interference RNA (siRNA) that specifically disrupted HIP14 expression (Figures 5B and Supplemental Figure S5). Next, we examined whether disruption of HIP14 expression altered trafficking of PSD-95 and GAD65, two neuronal proteins that rely on palmitoylation for targeting to post- and presynaptic sites, respectively (Craven et al., 1999; Kanaani et al., 2002). Remarkably, neurons transfected with HIP14 siRNA showed significant reduction in clustering of endogenous PSD-95 (Figures 5D–5F). In contrast, clustering of SAP-102, a nonpalmitoylated synaptic protein closely related to PSD-95, was not affected by HIP14 siRNA expression. In addition to altered localization of PSD-95, HIP14 siRNA significantly reduced axonal clustering of GFP-tagged GAD65 (Supplemental Figure S5 [http://www.neuron.org/cgi/content/full/44/6/977/DC1/]). These results establish that HIP14 is critical for the trafficking of acylated proteins targeted to both pre- and postsynaptic sites.

Discussion

In this study, we have identified HIP14 as a mammalian palmitoyl transferase that confers multiple substrate specificity. We demonstrate that HIP14 influences palmitoylation-dependent sorting and localization of acylated proteins in heterologous cells and neurons. Remarkably, HIP14-induced palmitoylation of diverse neuronal proteins sorted to both pre- and postsynaptic sites. The altered clustering of PSD-95 and GAD65 in neurons lacking HIP14 supports an in vivo role for this enzyme in protein palmitoylation. Another important finding of this study is that htt is also subject to palmitoylation by HIP14.

Although characterization of the kinetics of this enzyme has not been established, the ability of purified HIP14 to catalyze the transfer of palmitate on specific cysteine residues palmitoylated in vivo strongly supports its action as a palmitoyl transferase. Palmitoylated sequences modified by HIP14 lack a conserved consensus sequence and can be found at the N terminus or at internal sites. This finding is in contrast to enzymes involved in other lipid modifications, such as myristoylation and prenylation, which require a more defined consensus sequence located either at the N terminus or C terminus of modified proteins, respectively (El-Husseini and Bredt, 2002; Linder and Deschenes, 2004; Smotrys and Linder, 2004).

Previous investigations indicate that palmitoylation may occur at many cellular sites, including the cytosol, plasma membrane, Golgi/ER, and synaptic membranes (Resh, 1999; Smotrys and Linder, 2004). In this study, we show that HIP14 is a palmitoyl transferase that is mainly localized to the Golgi. Enrichment of HIP14 and other putative palmitoyl transferases such as GODZ and ZDHHC8 in the Golgi (Keller et al., 2004; Mukai et al., 2004) suggests that this compartment is a major site for palmitoylation. Importantly, several proteins examined in this study, including SNAP-25, synaptotagmin I, GAD65 and GAP-43, traffic through the Golgi (El-Husseini and Bredt, 2002; Gonzalo and Linder, 1998; Ka-

GFP in vesicle-like structures (arrowheads) present in the cytoplasm. Inverse color time-lapse images are shown. a, axon; g, Golgi apparatus; m, mitochondria, n, nucleus; s, dendritic spine. Scale bars, 500 nm (A); 833 nm (B); 250 nm (C and D); 150 nm (E); 200 nm (F); 500 nm (G); 10 μm (H and I). Magnified panels in (J) and (K), 1 μm.

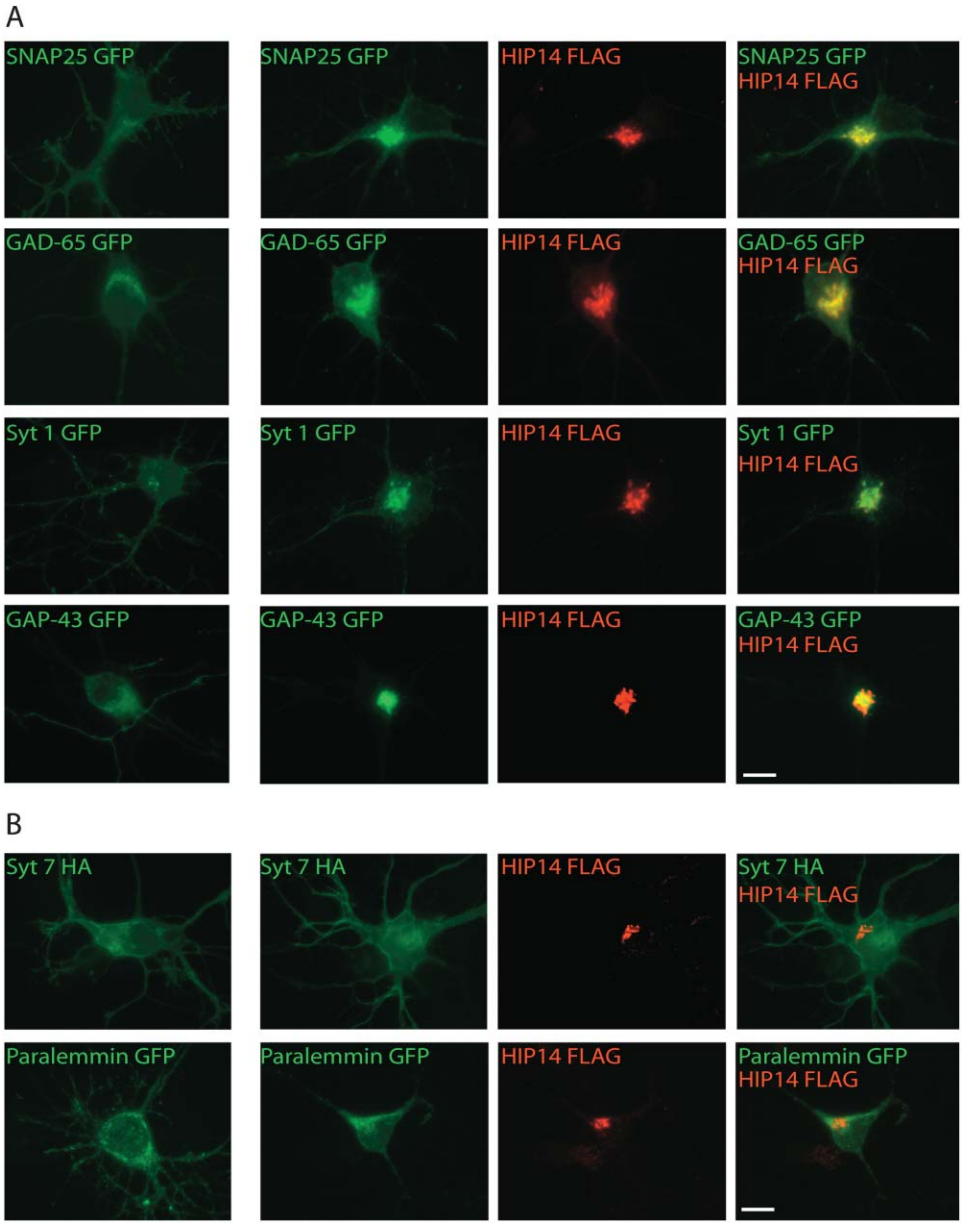

Figure 4. HIP14 Modulates Trafficking of Palmitoylated Proteins in Neurons

(A and B) GFP fusion proteins of SNAP-25, GAD65, synaptotagmin I (Syt 1), GAP-43, paralemmin, and HA-tagged synaptotagmin VII (Syt 7 HA) were transfected into cultured neurons (DIV 4) alone (left panels) or with a FLAG-tagged HIP14 (HIP14-FLAG; right panels). Overexpression of HIP14 enhances perinuclear accumulation of SNAP-25 GFP, GAD65 GFP, Syt 1 GFP, and GAP-43 GFP. In contrast, HIP14 did not alter the distribution of paralemmin GFP or Syt 7 HA. Scale bars, 10 μm.

naani et al., 2002; Resh, 1999; Smotrys and Linder, 2004; Sudhof, 2002). Thus, acylation of some of the analyzed proteins may occur in this compartment.

Our EM analysis revealed that HIP14 is mainly found associated with the cytosolic side of vesicles present in the cytoplasm. HIP14 immunogold particles were also detected at the plasma membrane and dendritic spines. Further evidence for the enrichment of HIP14 in vesicular structures trafficking in the cytosol was revealed by time-lapse imaging of cells expressing HIP14 GFP. The association of HIP14 with several vesicular compartments that may include recycling and late endosomes indicates that this enzyme acts at multiple subcellular locations. However, the ability of HIP14 to modulate acylation of cytosolic proteins such as PSD-95 is intriguing. Previous studies show that PSD-95 and htt associate with vesicular membranes (DiFiglia et al., 1995; El-Husseini et al., 2000; Velier et al., 1998). In addition, vesicular trafficking of PSD-95 to a perinuclear compartment is palmitoylation dependent and can be blocked by agents that disrupt the Golgi (El-Husseini et al., 2000). The detection of HIP14 on the cytosolic side of vesicular structures suggests that HIP14 may directly modify PSD-95 in the cytoplasm or on vesicles containing HIP14.

A recent report identified ski as an acyl-transferase in-

Table 1. Summary of Changes in the Localization of Palmitoylated Proteins in the Presence of HIP14 in Both COS Cells and Neurons

(A) HIP14 induces redistribution of a subset of palmitoylated proteins. The effects on palmitoylated proteins require the presence of cysteines modified by palmitate.

	COS Cells		Neurons	
	Enhanced Perinuclear Accumulation	Colocalization with HIP 14	Enhanced Perinuclear Accumulation	Colocalization with HIP 14
PSD-95-GFP	+++	C	+++	C
PSD-95-C3,5S-GFP	–	N	–	N
SNAP-25-GFP	+++	C	+++	C
SNAP-25-Palm mut GFP	–	N	–	N
GAP-43-GFP	+++	C	+++	P
Synaptotagmin I-GFP	++	C	+++	C
GAD65-GFP	++	C	+++	C
Synaptotagmin VII-HA	–	N	–	N
Paralemmin-GFP	–	P	–	P
PSD-95-prenyl-GFP	–	P	–	P

(B) Sequences of the palmitoylated motifs of proteins analyzed.

Protein	Palmitoylation Motif	Location
SNAP-25	LGKFCGLCVCPCNKLKSSDA	Internal
PSD-95	MDCLCIVTTKKY	Amino terminus
GAP-43	MLCCMRRTKQV	Amino terminus
Synaptotagmin I	VVTCCFCVCKKCL	Internal
GAD65	ARAWCQVAQKFTGGIGNKLCALLYG	Internal
Synaptotagmin VII	VTIVLCGLCHWCQRKLG	Internal
1ck	MGCVCSSNPEDDWME	Amino terminus
H-Ras	GPGCMSCKCVLS	Carboxyl terminus
Paralemmin	DMKKHRCKCCSIM	Carboxyl terminus

C, colocalized; N, not colocalized; P, partially colocalized

volved in palmitoylation of proteins within the lumen of the secretory pathway (Chamoun et al., 2001). In contrast, HIP14 appears to mediate palmitoylation of several intracellular proteins trafficking through a Golgi-dependent vesicular pathway, most likely at the cytosolic side of the membrane. These findings suggest the existence of at least two families of PATs that regulate acylation of intracellular and secreted proteins.

It is intriguing that HIP14 induced palmitoylation and altered trafficking of several unrelated neuronal proteins. These results suggest that HIP14 is a major PAT in neurons. However, the DHHC domain of HIP14 is conserved in 22 other DHHC-containing proteins that are present in both the mouse and the human genome (Smotrys and Linder, 2004). It is as yet unknown whether these proteins are functionally redundant palmitoyl transferases or whether they are differentially localized and specialized in the palmitoylation of a subset of proteins.

Experimental Procedures

Constructs, cDNA Cloning, and Mutagenesis

Full-length HIP14 was subcloned into pCI-neo as described earlier (Singaraja et al., 2002). HIP14 GFP was generated by inserting EGFP (Clontech, CA) at the C terminus, and HIP14-Flag was generated by PCR using a reverse primer containing FLAG sequence. HIP14ΔDHHC was generated by deletion of nucleotides encoding amino acids 440–487. Construction of GFP fusion proteins of wild-type and mutant forms of synaptotagmin I, SNAP-25, GAD65, and PSD-95 were generated by PCR and subcloned into the HindIII and EcoRI sites in-frame with GFP in pEGFP-N3 (Clontech). Wild-type and palmitoylation mutant GST-SNAP-25 fusion proteins were PCR amplified and subcloned into EcoRI/SalI of pGEX-6P3 (Amersham Biosciences, UK). Synaptotagmin I GST fusion constructs were subcloned into BamHI/SalI of pGEX-6P3. HIP14-GST was generated by insertion of full-length HIP14 cDNA in-frame with GST into pGEX-6P3 at the XmaI site. For production of 6× His-htt, sequences corresponding to amino acids 1–548 of htt were subcloned into the EcoRI and HindIII sites of pTrcB (GIBCO-Invitrogen, Calsbad, CA). For the generation of GST fusion proteins of other acylated proteins, nucleotide sequences corresponding to the acylated motifs of paralemmin (amino acids 364–383), lck (amino acids 1–20), synaptotagmin VII (amino acids 25–44), and H-Ras (amino acids 169–188) were subcloned into the BamHI and XhoI sites of pGEX-4T1 (Amersham). PSD-95 (1-PDZ3) in pGEX-2T was a gift from Dr. David Bredt (University of California at San Francisco, CA). All constructs were verified by DNA sequencing.

Cell Culture, Transfection, and Time-Lapse Imaging

COS cells and hippocampal and cortical neurons were cultured as described earlier (Craven et al., 1999; El-Husseini et al., 2000). Neuronal cultures were maintained in neurobasal media (GIBCO-Invitrogen) supplemented with B27, penicillin, streptomycin, and L-glutamine. For transient expression, both COS cells and 4 days in vitro (DIV) neurons were transfected with Lipofectamine 2000 (GIBCO-Invitrogen) according to the manufacturer's protocol and were stained 8–14 hr later. For time-lapse imaging, COS cells were transfected and images were collected 10 hr posttransfection using a 63× oil objective affixed to a Zeiss inverted light microscope and Axiovision software. While images were acquired, cells were kept in a 37°C chamber, supplemented with 5% carbon dioxide. Images were collected every 3 s for a total time of 3 min.

Immunofluorescence

Cells were washed in phosphate-buffered saline (PBS) (20 mM NaH_2PO_4, 0.9% NaCl, pH 7.4), fixed in 4% paraformaldehyde in PBS, and permeabilized in 0.3% Triton X-100, 1% paraformaldehyde. For immunofluorescence, primary antibodies were incubated in 2% NGS in PBS for 1 hr at room temperature. Cells were washed in PBS between each incubation followed by incubation with appropriate secondary antibodies conjugated to Alexa 488 and Alexa 568. Primary antibodies used include mouse monoclonal antibodies recognizing α-adaptin, Rab5, and Rab8 (Transduction Laboratories), GM-130 (BD Biosciences, Palo Alto, CA), GST and actin (Santa Cruz

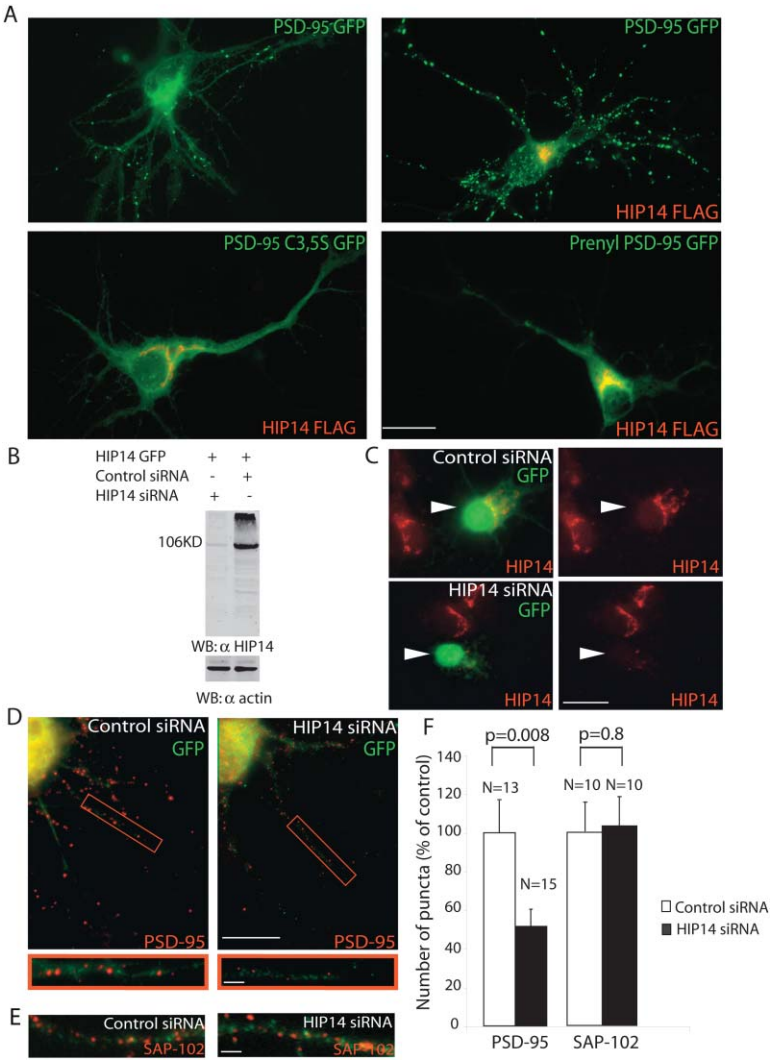

Figure 5. Manipulation of Endogenous Expression of HIP14 Alters Clustering of PSD-95 in Neurons

(A) HIP14 enhances palmitoylation-dependent clustering of PSD-95. Cultured hippocampal neurons (DIV 4) were transfected with the indicated constructs. Twelve hours post-transfection, clusters of wild-type PSD-95 GFP can be observed. In the presence of HIP14-FLAG, PSD-95 GFP clustering was enhanced. HIP14-FLAG did not alter trafficking of either the palmitoylation-deficient form (PSD-95 GFP C3,5S) or a mutant form of PSD-95 containing a prenyl motif (PSD-95 GFP Prenyl). (B–F) Blocking endogenous expression of HIP14 reduces clustering of PSD-95. (B) Western blot analysis of COS cells transfected with HIP14 GFP and either with HIP14 specific small interference RNA (HIP14 siRNA) or scrambled siRNA (Control siRNA) and then probed with antibodies against GFP (top panel) and actin (bottom panel). Analysis shows that HIP14 siRNA blocks expression of HIP14 GFP. (C) Hippocampal neurons (DIV 7) were transfected with GFP and either with HIP14 siRNA or control siRNA. At DIV 10, neurons were fixed and stained with antibodies against HIP14. Loss of HIP14 staining in neurons transfected with HIP14 siRNA (bottom panels; arrowheads) but not control siRNA (top panels; arrowheads). (D and E) HIP14 siRNA reduces clustering of (D) PSD-95 but not (E) SAP-102. (F) Summary of changes in the number of puncta of PSD-95 and SAP-102 in the dendrites of neurons expressing HIP14 siRNA compared to neurons expressing control siRNA. Scale bars, 10 μm (A, C, and D). Enlarged panels in (D) and (E), 1 μm.

Biotechnology, Inc. CA), PSD-95 (Affinity Bioreagents. Inc., CO), huntingtin antibody 2166 (Chemicon, CA), and goat polyclonal antibodies against Rab7 (Santa Cruz). Rabbit polyclonal antibodies against GFP (Clontech Laboratories Inc., CA) were also used. Rabbit polyclonal antibodies against HIP14 have been described previously (Singaraja et al., 2002). Guinea pig antibody against SAP102 was a gift from Dr. David Bredt (University of California at San Francisco, CA).

Electron Microscopy

Electron microscopy on HIP14 in the brain was performed as previously described (Singaraja et al., 2002). Ultrasmall colloidal gold conjugated secondary antibody (Aurion, Wageningen, The Netherlands) was used. Following a postfixation with 2.5% glutaraldehyde, gold particles were intensified using the R-gent SE-EM silver enhancement kit (Aurion). Sections were further fixed with 0.5% OsO_4 in 0.1 M PB, dehydrated in ethanol and propylene oxide (1:1), and flat-embedded in Eponate 12 (Ted Pella, Redding, CA). Ultrathin sections (90 nm) were cut using a Leica Ultracut S ultramicrotome and were counterstained with 5% aqueous uranyl acetate for 5 min followed by lead citrate for 5 min. Thin sections were examined using a HITACHI H-7500 electron microscope.

Cell Radiolabeling and Immunoprecipitation

COS cells were labeled with 1 mCi/ml [^{3}H]palmitate (57 Ci/mmol; Perkin Elmer Life Sciences, Inc.) for 3 hr while expressing the transfected proteins. Labeled cells were washed with ice-cold PBS and resuspended in 0.1 ml of lysis buffer containing TEE (50 mM Tris-HCl [pH 7.4], 1 mM EDTA, 1 mM EGTA), 150 mM NaCl, and 1% SDS. Triton X-100 (1%) was added to neutralize SDS in a final volume of 0.5 ml. Insoluble material was removed by centrifugation at 14,000 rpm for 10 min at 4°C. For immunoprecipitation, samples were incubated with SNAP-25 monoclonal antibodies for 1 hr at 4°C. After addition of 20 μl protein G sepharose beads (Pharmacia), samples were incubated for 1 hr at 4°C. Immunoprecipitates were washed three times with buffer containing TEE, 150 mM NaCl, and 1% Triton X-100, boiled in SDS-PAGE sample buffer with 1 mM DTT for 2 min, and separated by SDS-PAGE and dried under vacuum. Gels were exposed to Hyper Film (Amersham) with intensifying screens at −80°C for 3–20 days.

Expression and Purification of Fusion Proteins

GST fusion proteins were produced in *E. coli* using the pGEX 6p3 expression system (Amersham) and isolated using Glutathione Sepharose 4B (Amersham) from clarified cell lysates. The substrates were dialyzed and then eluted with 20 mM Glutathione. GST-HIP14 was purified in the presence of bovine liver lipids with no detergent to maintain proper protein folding. To generate a free N terminus of PSD-95, GST-PSD-95 protein was cleaved using thrombin (50 mM Tris-HCl [pH 8.0], 150 mM NaCl, 2.5 mM $CaCl_2$, 0.1% 2-mercaptoethanol). His-tagged htt protein was purified from DH5α with Ni-NTA magnetic agarose beads (Qiagen).

Immunoprecipitation of HIP14 GFP

Transfected COS cells were sonicated for 15 s in TEEN buffer (50 mM Tris-HCl [pH 7.4], 1 mM EDTA, 1 mM EGTA, 150 mM NaCl), and

insoluble material was removed by centrifugation at 14,000 rpm for 10 min at 4°C. Supernatants were incubated with anti-GFP antibody (10 μl) for 1 hr at 4°C. Protein A Sepharose 4 Fast Flow beads (50 μl) (Amersham) were added, and samples were incubated for 1 hr at 4°C. Immunoprecipitates were washed twice with buffer containing TEEN and 150 mM NaCl and then were subjected to in vitro palmitoylation assays described below.

Synthesis of Palmitoyl CoA

[^{3}H]palmitoyl-CoA, [^{3}H]myristoyl-CoA, and palmitoyl-CoA were synthesized enzymatically from [9,10-^{3}H(N)]palmitic acid (5 mCi/ml; Perkin Elmer Life Sciences), [9,10-^{3}H(N)]myristic acid (1mCi/ml; Perkin Elmer Life Sciences), and palmitic acid (Sigma-Aldrich), respectively. Synthesis components also included co-enzyme A (CoA), ATP, and acyl-CoA synthase (Sigma-Aldrich). Synthesized products were purified as previously described (Dunphy et al., 1996). Synthesized [^{3}H]palmitoyl-CoA and [^{3}H]myristoyl-CoA were subjected to TLC (TLC aluminium sheet, silica gel, EM Science, Germany) to determine the efficiency. Ninhydrin staining was used for the detection of synthesized nonradiolabeled palmitoyl-CoA. The synthesis was highly efficient, with >95% conversion of acid to fatty acid-CoA. Specific activity for [^{3}H]palmitoyl-CoA was 60 Ci/mmol and for [^{3}H]myristoyl-CoA was 30Ci/mmol.

Palmitoylation Assay

Palmitoylation reaction (60 μl) contained 5 μCi of [^{3}H]palmitoyl-CoA, 0.33 μg/μl substrate protein, 1 mM ATP, 50 mM MES, pH 6.4, 0.2 mg/ml bovine liver lipids, and either 20 μl of COS cell lysates expressing HIP14, immunoprecipitated HIP14 GFP, or 0.5 μg of purified HIP14-GST as described in results. After 15 min incubation at 37°C, sample buffer with final concentration of 5 mM DTT was added and samples were subjected to SDS-PAGE analysis.

HIP14 siRNA

HIP14 siRNA primers were annealed and inserted into the HindIII/BglII sites of pSUPER vector (Oligo Engine). Primers used to generate HIP14 siRNA are as follows. Complementary oligonucleotides: 5′-GATCCCCGGAGATACAAGCACTTTAATTCAAGAGATTAAAGTGCTTGTATCTCCTTTTTGGAAA-3′, and 5′-AGCTTTTCCAAAAAGGAGATACAAGCACTTTAATCTCTTGAATTAAAGTGCTTGTATCTCCGGG-3′ (corresponding to nucleotides 2039–2057 of rat HIP14 mRNA). Primers used to generate scrambled siRNA (control siRNA): 5′-GATCCCCGATAAGAACAGCGGCTATATTCAAGAGATATAGCCGCTGTTCTTATCTTTTTA-3′ and 5′-AGCTTAAAAAGATAAGAACAGCGGCTATATCTCTTGAATATAGCCGCTGTTCTTATCGGGGATCGGG -3′. The specificity of HIP14 siRNA was tested both against exogenously expressed HIP14 in COS cells and endogenous HIP14 in cultured hippocampal and cortical neurons.

Imaging and Analysis

Images were acquired on a Zeiss Axiovert M200 motorized microscope by using a monochrome 14 bit Zeiss Axiocam HR charge-coupled device camera at 1300 × 1030 pixels. Exposure times were individually adjusted to yield an optimum immunofluorescent brightness without saturation. Images were analyzed in Northern Eclipse (Empix Imaging, Missasauga, Canada). Briefly, images were processed at a constant threshold level (of 32,000 pixel values) to create a binary image, which was multiplied with the original image by using Boolean image arithmetics. An observer blind to the identity of proteins examined performed analysis in protein clustering upon expression of siRNA. For analysis of protein clustering, dendrites of the cell of interest were outlined using a combination of the GFP fluorescence signal and differential interference contrast bright-field images. Puncta were defined as sites of intensities at least twice the dendritic background. The number of dendritic puncta per unit dendritic length was measured. The two-tailed two-sample unequal variance Student's t test was used to compare the average number of puncta per unit length between experimental groups. For analysis of clustering of GAD65 GFP, the intensity of axonal clusters was determined. This was done by tracing three to four representative sections of axons. For each cell, the average intensity of axonal puncta versus axonal background was used to calculate the degree of clustering of GAD65. Results were analyzed by a Student's t test using a two-tailed distribution and two-sample unequal variance.

Acknowledgments

We thank Dr. Srikanth Dakoji and Kimberly Gerrow for their technical assistance and comments on the manuscript. This work was supported by grants to A.E.-H. and M.R.H. from the Canadian Institutes for Health Research (CIHR), the infrastructure unit from the Michael Smith Foundation for Health Research (MSFHR), and the High Q foundation. This work is also supported by grants from the EJLB foundation (to A.E.-H.), the Huntington's Disease Society of America and The Jack and Doris Brown Foundation (to M.R.H.). A.E.-H. is a CIHR new investigator, MSFHR Scholar, and University Distinguished Scholar. M.R.H. is a Killam University Professor and holds a Canada Research Chair in Human Genetics. K.H. is supported by a CIHR training award, A.Y. is supported by an MSFHR postdoctoral fellowship, and B.H. is supported by a fellowship from BC Children's Hospital Research Institute.

Received: August 20, 2004
Revised: October 13, 2004
Accepted: November 11, 2004
Published: December 15, 2004

References

Chamoun, Z., Mann, R.K., Nellen, D., von Kessler, D.P., Bellotto, M., Beachy, P.A., and Basler, K. (2001). Skinny Hedgehog, an acyltransferase required for palmitoylation and activity of the Hedgehog signal. Science *293*, 2080–2084.

Chapman, E.R., Blasi, J., An, S., Brose, N., Johnston, P.A., Sudhof, T.C., and Jahn, R. (1996). Fatty acylation of synaptotagmin in PC12 cells and synaptosomes. Biochem. Biophys. Res. Commun. *225*, 326–332.

Craven, S.E., El-Husseini, A.E., and Bredt, D.S. (1999). Synaptic targeting of the postsynaptic density protein PSD-95 mediated by lipid and protein motifs. Neuron *22*, 497–509.

Da Silva, J.S., and Dotti, C.G. (2002). Breaking the neuronal sphere: regulation of the actin cytoskeleton in neuritogenesis. Nat. Rev. Neurosci. *3*, pp. 694–704.

DiFiglia, M., Sapp, E., Chase, K., Schwarz, C., Meloni, A., Young, C., Martin, E., Vonsattel, J.P., Carraway, R., Reeves, S.A., et al. (1995). Huntingtin is a cytoplasmic protein associated with vesicles in human and rat brain neurons. Neuron *14*, 1075–1081.

Dunphy, J.T., Greentree, W.K., Manahan, C.L., and Linder, M.E. (1996). G-protein palmitoyltransferase activity is enriched in plasma membranes. J. Biol. Chem. *271*, 7154–7159.

El-Husseini, A.E., and Bredt, D.S. (2002). Protein palmitoylation: a regulator of neuronal development and function. Nat. Rev. Neurosci. *3*, 791–802.

El-Husseini, A.E., Craven, S.E., Chetkovich, D.M., Firestein, B.L., Schnell, E., Aoki, C., and Bredt, D.S. (2000). Dual palmitoylation of PSD-95 mediates its vesiculotubular sorting, postsynaptic targeting, and ion channel clustering. J. Cell Biol. *148*, 159–172.

El-Husseini, A.E., Schnell, E., Dakoji, S., Sweeney, N., Zhou, Q., Prange, O., Gauthier-Campbell, C., Aguilera-Moreno, A., Nicoll, R.A., and Bredt, D.S. (2002). Synaptic strength regulated by palmitate cycling on PSD-95. Cell *108*, 849–863.

Fukuda, M., Kanno, E., Ogata, Y., and Mikoshiba, K. (2001). Mechanism of the SDS-resistant synaptotagmin clustering mediated by the cysteine cluster at the interface between the transmembrane and spacer domains. J. Biol. Chem. *276*, 40319–40325.

Gauthier-Campbell, C., Bredt, D.S., Murphy, T.H., and El-Husseini, A.E.-D. (2004). Regulation of dendritic branching and filopodia formation in hippocampal neurons by specific acylated protein motifs. Mol. Biol. Cell *15*, 2205–2217.

Gonzalo, S., and Linder, M.E. (1998). SNAP-25 palmitoylation and plasma membrane targeting require a functional secretory pathway. Mol. Biol. Cell *9*, 585–597.

Heindel, U., Schmidt, M.F., and Veit, M. (2003). Palmitoylation sites and processing of synaptotagmin I, the putative calcium sensor for neurosecretion. FEBS Lett. *544*, 57–62.

Hess, D.T., Slater, T.M., Wilson, M.C., and Skene, J.H. (1992). The

25 kDa synaptosomal-associated protein SNAP-25 is the major methionine-rich polypeptide in rapid axonal transport and a major substrate for palmitoylation in adult CNS. J. Neurosci. *12*, 4634–4641.

Kanaani, J., El-Husseini, A.E., Aguilera-Moreno, A., Diacovo, J.M., Bredt, D.S., and Baekkeskov, S. (2002). A combination of three distinct trafficking signals mediates axonal targeting and presynaptic clustering of GAD65. J. Cell Biol. *158*, 1229–1238.

Kang, R., Swayze, R., Lise, M.F., Gerrow, K., Mullard, A., Honer, W.G., and El-Husseini, A.E. (2004). Presynaptic trafficking of synaptotagmin I is regulated by protein palmitoylation. J. Biol. Chem., in press. Published online September 7, 2004.

Keller, C.A., Yuan, X., Panzanelli, P., Martin, M.L., Alldred, M., Sassoe-Pognetto, M., and Luscher, B. (2004). The gamma2 subunit of GABA(A) receptors is a substrate for palmitoylation by GODZ. J. Neurosci. *24*, 5881–5891.

Kutzleb, C., Sanders, G., Yamamoto, R., Wang, X., Lichte, B., Petrasch-Parwez, E., and Kilimann, M.W. (1998). Paralemmin, a prenylpalmitoyl-anchored phosphoprotein abundant in neurons and implicated in plasma membrane dynamics and cell process formation. J. Cell Biol. *143*, 795–813.

Lee, S.H., and Sheng, M. (2000). Development of neuron-neuron synapses. Curr. Opin. Neurobiol. *10*, 125–131.

Linder, M.E., and Deschenes, R.J. (2004). Model organisms lead the way to protein palmitoyltransferases. J. Cell Sci. *117*, 521–526.

Mukai, J., Liu, H., Burt, R.A., Swor, D.E., Lai, W.S., Karayiorgou, M., and Gogos, J.A. (2004). Evidence that the gene encoding ZDHHC8 contributes to the risk of schizophrenia. Nat. Genet. *36*, 725–731.

Rathenberg, J., Kittler, J.T., and Moss, S.J. (2004). Palmitoylation regulates the clustering and cell surface stability of GABA(A) receptors. Mol. Cell. Neurosci. *26*, 251–257.

Resh, M.D. (1999). Fatty acylation of proteins: new insights into membrane targeting of myristoylated and palmitoylated proteins. Biochim. Biophys. Acta. *1451*, 1–16.

Roth, A.F., Feng, Y., Chen, L., and Davis, N.G. (2002). The yeast DHHC cysteine-rich domain protein Akr1p is a palmitoyl transferase. J. Cell Biol. *159*, 23–28.

Singaraja, R.R., Hadano, S., Metzler, M., Givan, S., Wellington, C.L., Warby, S., Yanai, A., Gutekunst, C.A., Leavitt, B.R., Yi, H., et al. (2002). HIP14, a novel ankyrin domain-containing protein, links huntingtin to intracellular trafficking and endocytosis. Hum. Mol. Genet. *11*, 2815–2828.

Smotrys, J.E., and Linder, M.E. (2004). Palmitoylation of intracellular signaling proteins: regulation and function. Annu. Rev. Biochem. *73*, 559–587.

Strittmatter, S.M., Fankhauser, C., Huang, P.L., Mashimo, H., and Fishman, M.C. (1995). Neuronal pathfinding is abnormal in mice lacking the neuronal growth cone protein GAP-43. Cell *80*, 445–452.

Sudhof, T.C. (2002). Synaptotagmins: why so many? J. Biol. Chem. *277*, 7629–7632.

Ueno, K. (2000). Involvement of fatty acid synthase in axonal development in mouse embryos. Genes Cells *5*, 859–869.

Velier, J., Kim, M., Schwarz, C., Kim, T.W., Sapp, E., Chase, K., Aronin, N., and DiFiglia, M. (1998). Wild-type and mutant huntingtins function in vesicle trafficking in the secretory and endocytic pathways. Exp. Neurol. *152*, 34–40.

Washbourne, P., Cansino, V., Mathews, J.R., Graham, M., Burgoyne, R.D., and Wilson, M.C. (2001). Cysteine residues of SNAP-25 are required for SNARE disassembly and exocytosis, but not for membrane targeting. Biochem. J. *357*, 625–634.